

Original Article

Spaceflight alters the gene expression profile of cervical cancer cells

Zhi-Jie Zhang, Yong-Qing Tong, Jia-Jia Wang, Cheng Yang, Guo-Hua Zhou, Yue-Hui Li, Ping-Li Xie, Jin-Yue Hu and Guan-Cheng Li

Abstract

Our previous study revealed that spaceflight induced biological changes in human cervical carcinoma Caski cells. Here, we report that 48A9 cells, which were subcloned from Caski cells, experienced significant growth suppression and exhibited low tumorigenic ability after spaceflight. To further understand the potential mechanism at the transcriptional level, we compared gene expression between 48A9 cells and ground control Caski cells with suppression subtractive hybridization (SSH) and reverse Northern blotting methods, and analyzed the relative gene network and molecular functions with the Ingenuity Pathways Analysis (IPA) program. We found 5 genes, *SUB1*, *SGEF*, *MALAT-1*, *MYL6*, and *MT-CO2*, to be up-regulated and identified 3 new cDNAs, termed *B4*, *B5*, and *C4*, in 48A9 cells. In addition, we also identified the two most significant gene networks to indicate the function of these genes using the IPA program. To our knowledge, our results show for the first time that spaceflight can reduce the growth of tumor cells, and we also provide a new model for oncogenesis study.

Key words Cervical carcinoma, oncogenesis, tumor suppressor, subtractive cDNA libraries, SSH

A complex environmental condition existed during spaceflight in which several interacting factors such as cosmic radiation, microgravity, and space magnetic fields may provoke stress responses, jeopardize genome integrity, and induce various biological changes in cells^[1-5]. Currently, a majority of studies on spaceflight focus on normal tissues and cells; however, little is known of the effects of spaceflight on abnormal cells such as cancer cells.

To investigate potential effects of space environment exposure on cancer cells, we examined the biological changes in Caski cells that experienced spaceflight aboard the “Shen Zhou IV” spaceship^[6]. After seven days in space, surviving cells were subcloned into 1440 cell lines. Of these, four cell lines were screened with cell proliferation assays, flow cytometry, soft agar

assays, and tumor formation experiments in nude mice. The 44F10 and 17E3 cell lines were selected because of their increased cell proliferation and tumorigenesis, whereas the 48A9 and 31F2 cell lines had obvious slower cytological events. In particular, 48A9 cells showed significantly diminished growth ability and decreased tumorigenesis *in vitro* and *in vivo* compared with ground control Caski cells. To further investigate 48A9 cells at the subcellular level, we examined the expression of 2747 tumor-associated genes in 48A9 Caski cells by DNA microarray analysis. The results indicated that genes differentially expressed in cells exposed to spaceflight were related to cell cycle, apoptosis, proliferation, and signal transduction.

Microarray is a powerful technique with which to identify possible ectopic gene expression; however, it has some disadvantages. For example, microarray cannot be used to detect unknown transcripts or to discriminate variant transcripts from previously characterized transcripts. Moreover, with only 2747 tumor-associated probe sets used in the study, our analysis reflected only a part of the altered gene expression patterns. In order to further understand the biological changes in 48A9 cells at the transcriptional

Authors' Affiliation: Cancer Research Institute, Xiangya School of Medicine, Central South University, Changsha, Hunan 410078, P. R. China

Corresponding Author: Guan-Cheng Li, Cancer Research Institute, Xiangya School of Medicine, Central South University, Changsha, Hunan 410078, P. R. China. Tel: +86-731-84805445; Fax: +86-731-82355042; Email: libsun@163.com.

doi: 10.5732/cjc.011.10174

level, we used an improved suppression subtractive hybridization (SSH) method to selectively determine differentially expressed genes^[7-9]. Using this method in 48A9 cells exposed to spaceflight, we successfully identified several genes to be significantly up-regulated, including Src homology 3 domain-containing guanine nucleotide exchange factor (*SGEF*), submergence-1 (*SUB1*), non-coding RNA metastasis-associated lung adenocarcinoma transcript 1 (*MALAT-1*), cytochrome c oxidase subunit 2 (*MT-CO2*), and myosin light chain 6 (*MYL6*), and identified three new putative genes. Furthermore, two most significant gene networks were identified using the Ingenuity Pathways Analysis (IPA) program. To our knowledge, our results show for the first time that spaceflight can reduce the growth of tumor cells, and we also provide a new model to study oncogenesis.

Materials and Methods

Cell culture

The human cervical carcinoma Caski cell strain was used as a ground control, and the 48A9 subclonal Caski cell strain^[6] was used for testing the effects of spaceflight. Both cell lines were maintained in Dulbecco's modified Eagle medium (DMEM) (Invitrogen, Carlsbad, CA, USA) containing 10% FBS and antibiotics in a humidified atmosphere of 5% CO₂ and 95% air at 37°C.

Cellular mRNA isolation

mRNA was directly extracted from ground control and 48A9 Caski cells and purified with the PolyATtract[®] mRNA isolation system kit (Promega Corporation, Madison, WI, USA) according to manufacturer's instruction. mRNA integrity was analyzed by gel electrophoresis.

SMART[™] cDNA synthesis

cDNAs were synthesized from 1 µg mRNA using super SMART[™] polymerase chain reaction (PCR) cDNA synthesis kit (Clontech, Mountain View, CA, USA) as described in the user manual. Briefly, a modified oligo (dT) primer primes the first-strand synthesis reaction. When reverse transcriptase (RT) reaches the 5' end of the mRNA, the enzyme's terminal transferase activity adds a few additional nucleotides, primarily deoxycytidine, to the 3' end of the cDNA. The SMART[™] oligonucleotide which has an oligo(G) sequence at its 3' end, base-pairs with the deoxycytidine stretch, creating an extended template. RT then switches templates and continues replicating to the end of the oligonucleotide. The smart anchor sequence and the poly A sequence serve as

universal priming sites for end-to-end cDNA amplification by long-distance PCR with advantage 2 polymerase mix (Clontech, Mountain View, CA, USA). The PCR products, SMART[™] cDNA, were purified with PCR purification kit (Qiagen, Shanghai, China) and used for the suppression subtractive hybridization experiment.

SSH

The PCR-selected cDNA subtraction kit was purchased from Clontech (Clontech, Mountain View, CA, USA) and used according to the manufacturer's instructions. In brief, cDNA products were digested with *Rsa* I. The digested 48A9 cell cDNA was then ligated with adapters provided in the kit. Ligation efficiency was determined by PCR. Two rounds of hybridization were performed using 48A9 cell cDNA as the tester and ground control cell cDNA as the driver. An additional two rounds of subtractive PCR were performed to enrich differential fragments. To evaluate the subtractive efficiency, the relative amount of glyceraldehyde-3-phosphate dehydrogenase (*GAPDH*) present in the subtracted and unsubtracted cDNA was determined by PCR amplification using the primers provided in the kit.

Construction of subtractive cDNA libraries

The second round subtractive PCR products were cloned into the pMD19-T vector (TaKaRa, Dalian, China). Ligation products were subsequently transformed into *E. coli* DH5α competent cells (TaKaRa, Dalian, China), plated on prepared LB agar plates containing 200 µg/mL ampicillin, 625 µmol/L IPTG, and 0.005% X-gal. After 12 h in the 37°C incubator, the presence of cDNA inserts was verified by PCR amplification using nested PCR primers supplied in the PCR-selected cDNA subtraction kit.

Reverse Northern blotting and sequencing

The differentially expressed genes were screened by reverse Northern blotting and identified by sequencing. Briefly, the recombinant clones including cDNA inserts were amplified by PCR using nested PCR primers with *Pfu* DNA polymerase (Promega, Madison, WI, USA). A total of 192 PCR products (2 µg) were denatured in 0.4 mol/L NaOH and spotted onto a nylon membrane (Millipore, Billerica, MA, USA) in duplicate. The cDNAs were cross-linked to the membrane by incubation at 80°C for 2 h. The membranes were hybridized in ExpressHyb[™] solution (Clontech, Mountain View, CA, USA) at 68°C for 18 h with equivalent specific activity of ³²P-labeled cDNA probes derived from 48A9 or ground control cells, followed by washing in a low stringency solution (2× SSC, 1% SDS; 3 times for 15 min) and

then a high stringency solution (0.1× SSC, 0.5% SDS; 3 times for 15 min) at 68°C. Finally, the membranes were exposed to X-film (Pierce, Woburn, MA, USA) for 48 h at -70°C. After scanning, the intensity of the hybridization signals was determined with Image J software provided by National Institutes of Health (NIH). Differentially expressed clones that were screened by reverse Northern dot blotting were sequenced and analyzed for homology to known sequences in the National Center of Biotechnology Information (NCBI) database.

Semi-quantitative RT-PCR

To further confirm the SSH results, total RNA was extracted from 48A9 and ground control cells with TRIzol reagent (Invitrogen, Carlsbad, CA, USA) according to the standard protocol. M-MuLV reverse transcriptase and oligo-dT primer (New England Biolabs, Ipswich, MA, USA) were used to synthesize cDNA. Finally, PCR amplification was performed using gene-specific primers. Semi-quantitative analysis of the mRNA level was achieved with 1% agarose gel electrophoresis.

Network and function analysis

The differentially expressed genes in 48A9 cells, which were identified by SSH and our previous microarray experiment^[6], were further analyzed using the online IPA program (<http://www.ingenuity.com>). Briefly, the up-regulated genes identified by SSH and up- and down-regulated genes identified by microarray were uploaded into IPA and were then mapped to the Ingenuity Pathways Knowledge base. The so-called focus genes were used for network generation and biological function and/or diseases analyses. Networks of these focus genes were algorithmically generated based on their connectivity. The functional analysis of a network identified the biological functions and/or diseases that were most significant to the genes in the network.

Statistical analyses

All data are presented as mean ± standard deviation (SD). Fisher's exact test was used to calculate a *P* value for the probability that each biological function and/or disease assigned to that network is due to chance alone. A value of *P* < 0.05 was considered statistically significant.

Results

Cells, mRNA, and SMARTTM cDNA analysis

The growth status of ground control and 48A9 cells

was the same as in our previous study^[6] (Figure 1A). Both the mRNA extracted from these cells and the cDNA generated were high quality according to typical band patterns (Figure 1B and C).

PCR identification of SSH

Though both the digested and undigested cDNA appeared smeared, the cDNA fragments generated by digestion with *Rsa* I were shorter than undigested cDNA (Figure 2A). Furthermore, comparing the intensity of PCR products amplified using one gene-specific primer (*GAPDH* 3' primer) and PCR primer 1 with using two gene-specific primers (*GAPDH* 3' primer and 5' primer) (Figure 2B), the ligation efficiency for the adaptors was greater than 50% (Figure 2D). Finally, the analysis of subtractive efficiency showed a reduction in the abundance of non-differentially expressed genes by SSH. *GAPDH* products could only be detected in the unsorted cDNA pool after 18 cycles of PCR amplification and in the subtracted cDNA pool after 28 cycles of PCR amplification, indicating a dramatic subtraction of commonly expressed genes in these samples (Figure 2C).

Construction and screen of a subtracted cDNA library

Of thousands of colonies, 300 cDNA clones were randomly picked, and plasmids were isolated and amplified by PCR with nested primers. As a result, 288 positive clones had PCR products with a length from 200 to 1200 bp. Figure 3A shows cDNA fragments of different lengths amplified by PCR from the isolated clones. To eliminate the false positive cDNA clones, a total of 192 clones with inserts were analyzed by reverse Northern blotting (Figure 3B), and the differential cDNA clones were identified by calculating gray values of hybridization signals using NIH Image J software. The cDNA clones with ratio (gray value of 48A9 probe/ground control probe) >2 were regarded as differentially expressed which represents the candidate genes up-regulated in 48A9 cells. At present, we have detected 12 cDNA clones expressed higher in 48A9 cells than in ground control cells.

Sequencing, homology searching, and semi-quantitative PCR

The genes identified in the 12 clones are summarized in Table 1. Sequencing analysis revealed that 5 of the 12 clones matched known genes in the GenBank/EMBL database, and 3 were predicted genes. The other 4 clones did not match any entries in the GenBank/EMBL database and may represent novel genes. The results of semi-quantitative PCR further

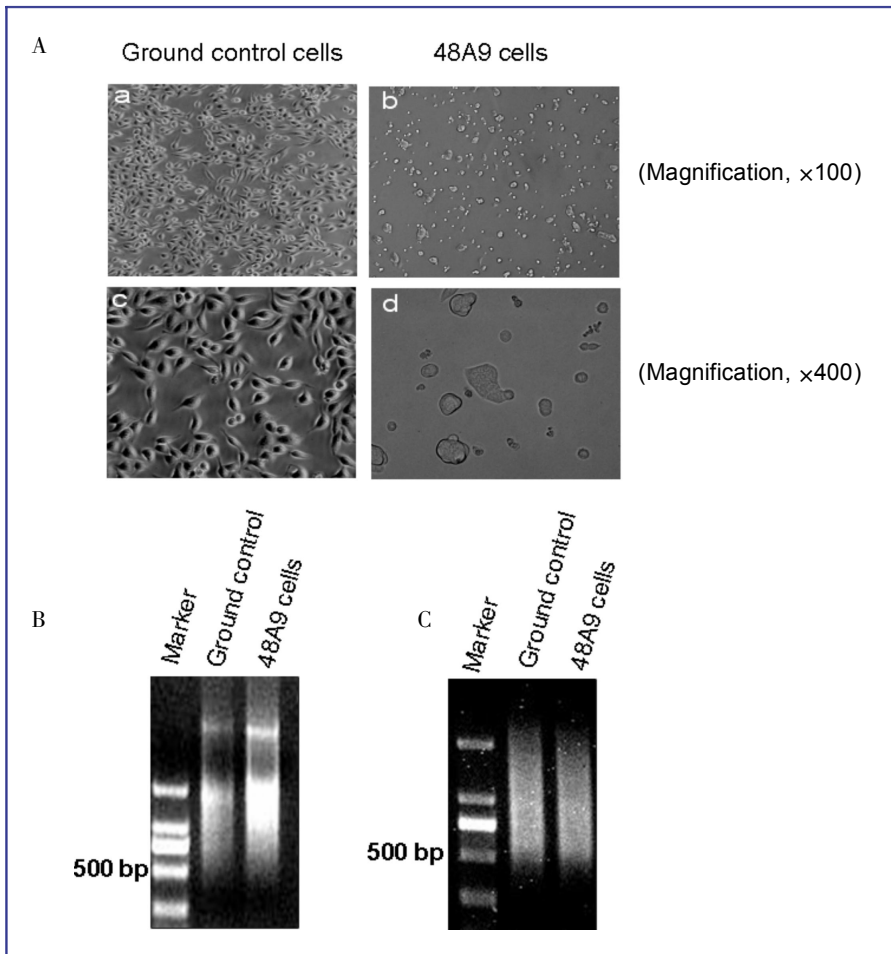


Figure 1. The growth status of cells and the high quality mRNAs and cDNAs. A, the images of ground control cells (a, c) and 48A9 cells (b, d). B, high integrity and purity of mRNAs. C, high quality cDNAs of ground control cells and 48A9 cells.

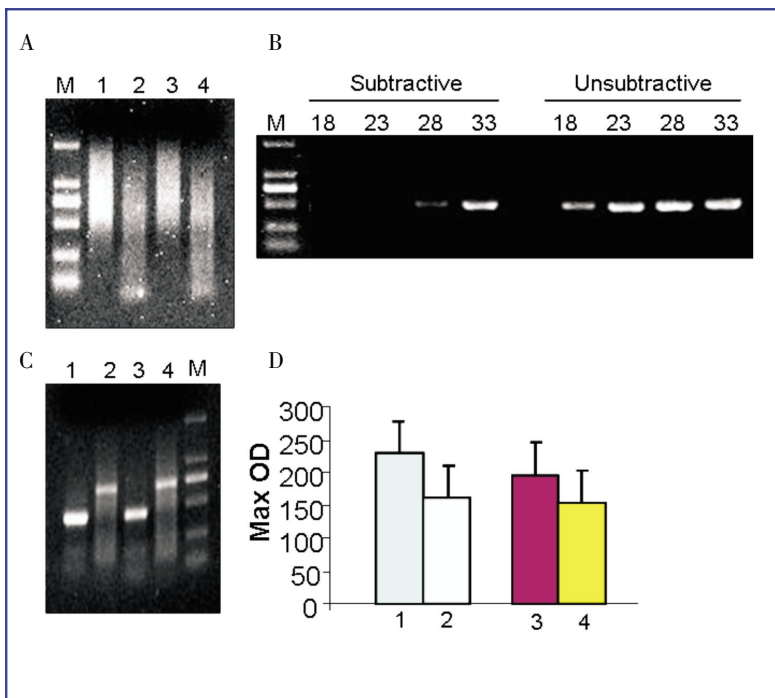


Figure 2. Results of suppression subtractive hybridization (SSH). A, analysis of *Rsa* I digestion. Lanes 1 and 3, SMART™ cDNA synthesis in ground control and 48A9 cells, respectively, before *Rsa* I digestion; lanes 2 and 4, SMART™ cDNA synthesis in ground control and 48A9 cells, respectively, after *Rsa* I digestion; M, DNA marker DL2000. B, reduction of *GAPDH* abundance by polymerase chain reaction (PCR)-select subtraction. PCR was performed on subtracted (18, 23, 28, 33 cycles) or unsubtracted (18, 23, 28, 33 cycles) secondary PCR products with the *GAPDH* 5' and 3' primers. Lane M, DNA marker DL2000. C and D, results of the ligation efficiency analysis. Lane 1, PCR products using Tester 1-1 (Adaptor 1-ligated) as the template and the *GAPDH* 3' and 5' primers. Lane 2, PCR products using Tester 1-1 (Adaptor 1-ligated) as the template, and the *GAPDH* 3' primer and PCR primer 1. Lane 3, PCR products using Tester 1-2 (Adaptor 2R-ligated) as the template, and the *GAPDH* 3' and 5' primers. Lane 4, PCR products using Tester 1-2 (Adaptor 2R-ligated) as the template, and the *GAPDH* 3' primer and PCR primer 1. Lane M, DNA marker DL2000.

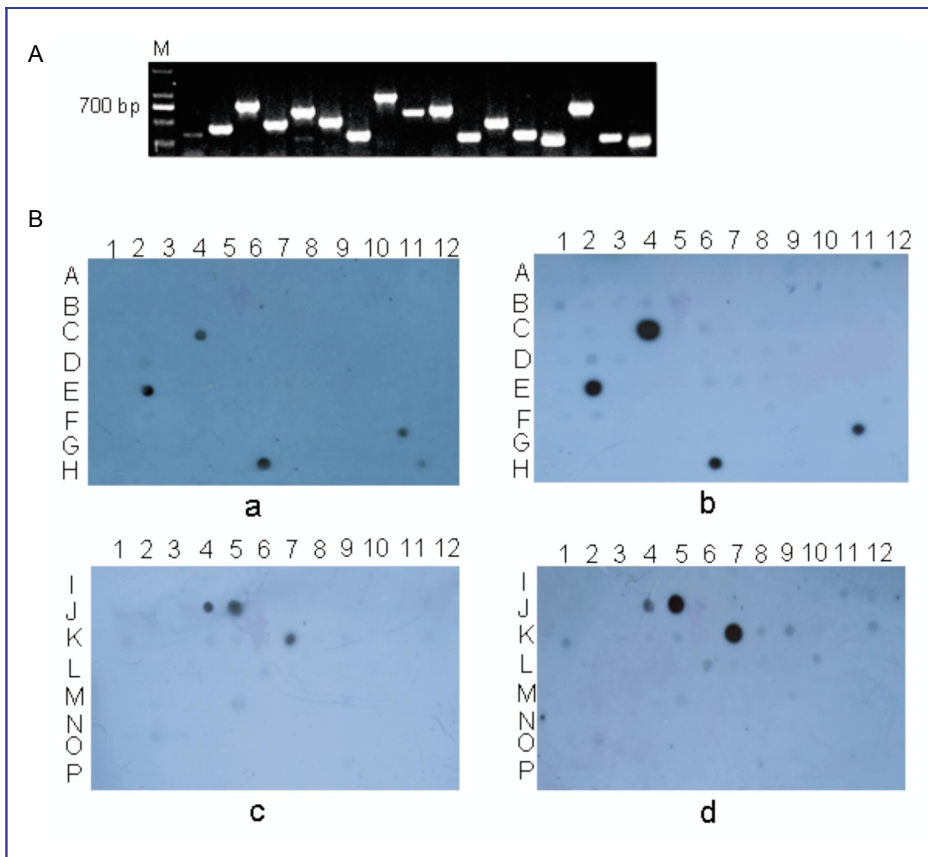


Figure 3. Construction and screening of a subtracted cDNA library. A, cDNA fragments of different lengths from colonies amplified by PCR. Lanes, randomly selected clones; lane M, DNA marker DL2000. B, screening differentially expressed cDNA clones by reverse Northern blotting. cDNA clones randomly picked from the subtracted library were dotted onto two nylon membranes and hybridized separately with ^{32}P -labeled cDNA probes prepared from ground control cell cDNA (a, c) and from 48A9 cell cDNA (b, d). Differentially expressed clones were selected for sequence analysis

Table 1. Genes differentially expressed between 48A9 and ground control Caski cells by suppression subtractive hybridization (SSH)

Clone	Size	Gene	GenBank number	Chromosome location	Relative ratio (48A9/control)
A2	762	<i>SUB1</i>	NM_006713.2	5p13.3	> 3
A9	320	<i>MT-CO2</i>	NC_001807.4	MT	> 3
B1	580	<i>MYL6</i>	NM_079423	12q13.2	> 3
F2	644	<i>MALAT-1</i>	NR_002819.1	11q13.1	> 3
G6	240	<i>SGEF</i>	NM_015595	3q25.2	> 3
B4	406	New sequence	NT_005612.15	3	> 3
B5	1185	New sequence	RP11-96F15	3p23	> 3
C4	751	New sequence	RP11-95H14	2q3	> 3

All identified cDNA sequences are >95% homologous to the known genes in the National Center of Biotechnology Information (NCBI) blast search database.

confirmed that expression of the 8 known and predicted genes was up-regulated in 48A9 cells (Figure 4).

Network and function analyses

The IPA program was used to gain insight into the potential functional implications of the spaceflight-induced changes in gene translation profiles in 48A9

cells. Genes up-regulated >2.0 fold or down-regulated <0.5 fold by microarray (Table 2) and up-regulated >3.0 by SSH were chosen for analysis. Under these criteria, 37 molecules were eligible for generating networks, and 35 molecules were qualified for functional analyses. As summarized in Table 3, the two most significant networks identified by IPA were related to cancer, with a score of 64 (Figure 5A), and cell morphology and cycle,

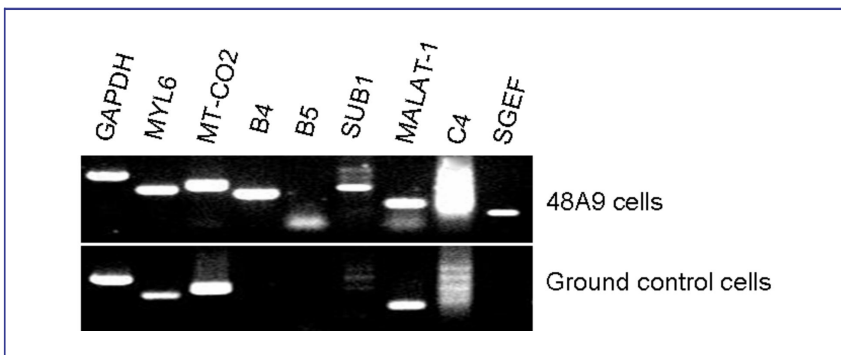


Figure 4. The result of semi-quantitative PCR. The lanes were *GAPDH* (internal control), *MYL6*, *MT-CO2*, *B4*, *B5*, *SUB1*, *MALAT-1*, *C4*, and *SGEF* genes, respectively. Compared to ground control cells, the expression levels of *MYL6*, *MT-CO2*, *B4*, *B5*, *SUB1*, *MALAT-1*, *C4*, and *SGEF* were up-regulated in 48A9 cells.

Table 2. Genes differentially expressed between 48A9 and ground control Caski cells by microarray

GenBank accession	Gene name	Cy5/Cy3 ratio
NM_001875	Homo sapiens carbamoyl-phosphate synthetase 1, <i>CPS1</i>	0.0744
NM_006799	Homo sapiens protease, serine 21, <i>PRSS21</i>	0.0877
NM_005567	Homo sapiens lectin, galactoside-binding, soluble, 3 binding protein, <i>LGALS3BP</i>	0.1987
NM_002888	Homo sapiens retinoic acid receptor responder 1, <i>RARRES1</i>	0.2108
NM_080733	Homo sapiens WAP four-disulfide core domain 2, <i>WFDC2</i>	0.2673
NM_000636	Homo sapiens superoxide dismutase 2, <i>SOD2</i>	0.2963
NM_003733	Homo sapiens 2'-5'-oligoadenylate synthetase-like, <i>OASL</i>	0.3394
NM_002447	Homo sapiens macrophage stimulating 1 receptor, <i>MST1R</i>	0.3663
NM_005564	Homo sapiens lipocalin 2, <i>LCN2</i>	0.3784
NM_007192	Homo sapiens suppressor of Ty 16 homolog, <i>SUPT16H</i>	0.4219
NM_001252	Homo sapiens tumor necrosis factor (ligand) superfamily, member 7, <i>TNFSF7</i>	0.4314
NM_002213	Homo sapiens integrin, beta 5, <i>ITGB5</i>	0.4486
NM_013282	Homo sapiens ubiquitin-like, containing PHD and RING finger domains 1, <i>UHRF1</i>	0.4564
NM_001809	Homo sapiens centromere protein A, <i>CENPA</i>	0.4613
NM_006034	Homo sapiens tumor protein p53 inducible protein 11	0.4643
NM_006569	Homo sapiens cell growth regulator with EF-hand domain 1, <i>CGREF1</i>	0.4747
NM_002466	Homo sapiens v-myb myeloblastosis viral oncogene homolog (avian)-like 2, <i>MYBL2</i>	0.4835
NM_005956	Homo sapiens formyltetrahydrofolate synthetase, <i>MTHFD1</i>	0.4939
NM_001254	Homo sapiens CDC6 cell division cycle 6 homolog, <i>CDC6</i>	0.4947
NM_002768	Homo sapiens procollagen (type III) N-endopeptidase, <i>PCOLN3</i>	2.0425
NM_002620	Homo sapiens platelet factor 4 variant 1, <i>PF4V1</i>	2.0552
NM_002705	Homo sapiens periplakin, <i>PPL</i>	2.1058
NM_002414	Homo sapiens CD99 antigen, <i>MIC2</i>	2.1294
NM_014599	Homo sapiens melanoma antigen family D 2, <i>MAGED2</i>	2.1429
NM_003365	Homo sapiens ubiquinol-cytochrome c reductase core protein 1, <i>UQCRC1</i>	2.1631
NM_000099	Homo sapiens cystatin C, <i>CST3</i>	2.1716
NM_000215	Homo sapiens Janus kinase 3, <i>JAK3</i>	2.1719
NM_003982	Homo sapiens solute carrier family 7 member 7, <i>SLC7A7</i>	2.3386
NM_002051	Homo sapiens GATA binding protein 3, <i>GATA3</i>	2.4381
NM_000362	Homo sapiens TIMP metalloproteinase inhibitor 3, <i>TIMP3</i>	2.4918
NM_004103	Homo sapiens PTK2B protein tyrosine kinase 2 beta, <i>PTK2B</i>	2.4970
NM_001924	Homo sapiens growth arrest and DNA-damage-inducible alpha, <i>GADD45A</i>	2.6718
NM_058242	Homo sapiens keratin 6C, <i>KRT6C</i>	3.0889
NM_001831	Homo sapiens clusterin, <i>CLU</i>	3.4840
NM_005009	Homo sapiens non-metastatic cells 4, <i>NME4</i>	5.7207
NM_000115	Homo sapiens endothelin receptor type B, <i>EDNRB</i>	7.1642

Table 3. The two most significant networks identified by the Ingenuity Pathways Analysis

ID	Molecules in network	Score	Number of focus molecules	Top functions
1	Akt, CD70, CDC6, CHMP1A, CLU, CST3, Cyclin A, E2f, EDNRB, ERK, GADD45A, GATA3, hCG, Histoneh3, ITGB5, JAK3, Jnk, KRT6A, LCN2, MAGED2, MST1R, MTHFD1, MYBL2, NFkB, PDGFBB, PF4V1, PTK2B, RNA polymerase II, SLC7A7, SOD2, SUB1, SUPT16H, TCR, UHRF1, UQCRC1	64	24	Cancer, nephrosis, renal and urological disease
2	OASL, PPL, PTPN11, RARRES1, RLN2, SGEF, SMPD1, TFAP2C, Timp, TIMP3, CTLA4, CTSH, ERBB2, HSD17B1, ICAM1, IFNG, IL1RN, LCN2, LGALS3BP, LRP8, MYBL2, NFkB, ACP, ADAMTS5, ALDH1A7, C19ORF10, CD14, CENPA, CGREF1, COL5A1, COL6A1, Tnf receptor, TP53I11	23	11	Cell morphology, cell cycle, embryonic development

All identified cDNA sequences are >95% homologous to the known genes in the National Center of Biotechnology Information (NCBI) blast search database.

with a score of 23 (Figure 5B). In addition, the top biological functions are shown in Figure 5C. As expected for data derived from our previous study^[6], the most represented functions in 48A9 cells were cell growth and proliferation (24 focus genes), cell morphology (13 focus genes), cell death (18 focus genes), and cancer (25 focus genes).

Discussion

Here, we report that by using a sensitive subtraction method, we identified new spaceflight-inducible genes in cancer cells that were not identified by microarray. These genes included transcriptional co-activator *SUB1*, *SGEF*, *MALAT-1*, cytoskeleton relative gene *MYL6*, and mitochondrial metabolism gene *MT-CO2*, as well as three new putative genes with unknown function. Moreover, by utilizing the IPA program and combining our previous microarray data, we identified the two most significant functional networks impacted by spaceflight-induced gene changes—the cancer network and the cell morphology and cycle network. These networks, which include cell signaling pathways such as the stress-activated protein kinase/c-Jun NH₂-terminal kinase (SAPK/JNK) pathway, mitogen-activated protein kinase (MAPK) pathway, and Akt pathway, as well as cell signaling molecules such as nuclear factor- κ B (NF- κ B), interferon gamma (IFNG), histone H3, and intercellular adhesion molecule 1 (ICAM1), may play an important role in controlling cell growth and maintaining cell morphology in spaceflight. These results provide important clues for further study of the influence of spaceflight on gene expression and oncogenesis.

SUB1 and its potential functions in 48A9 cells

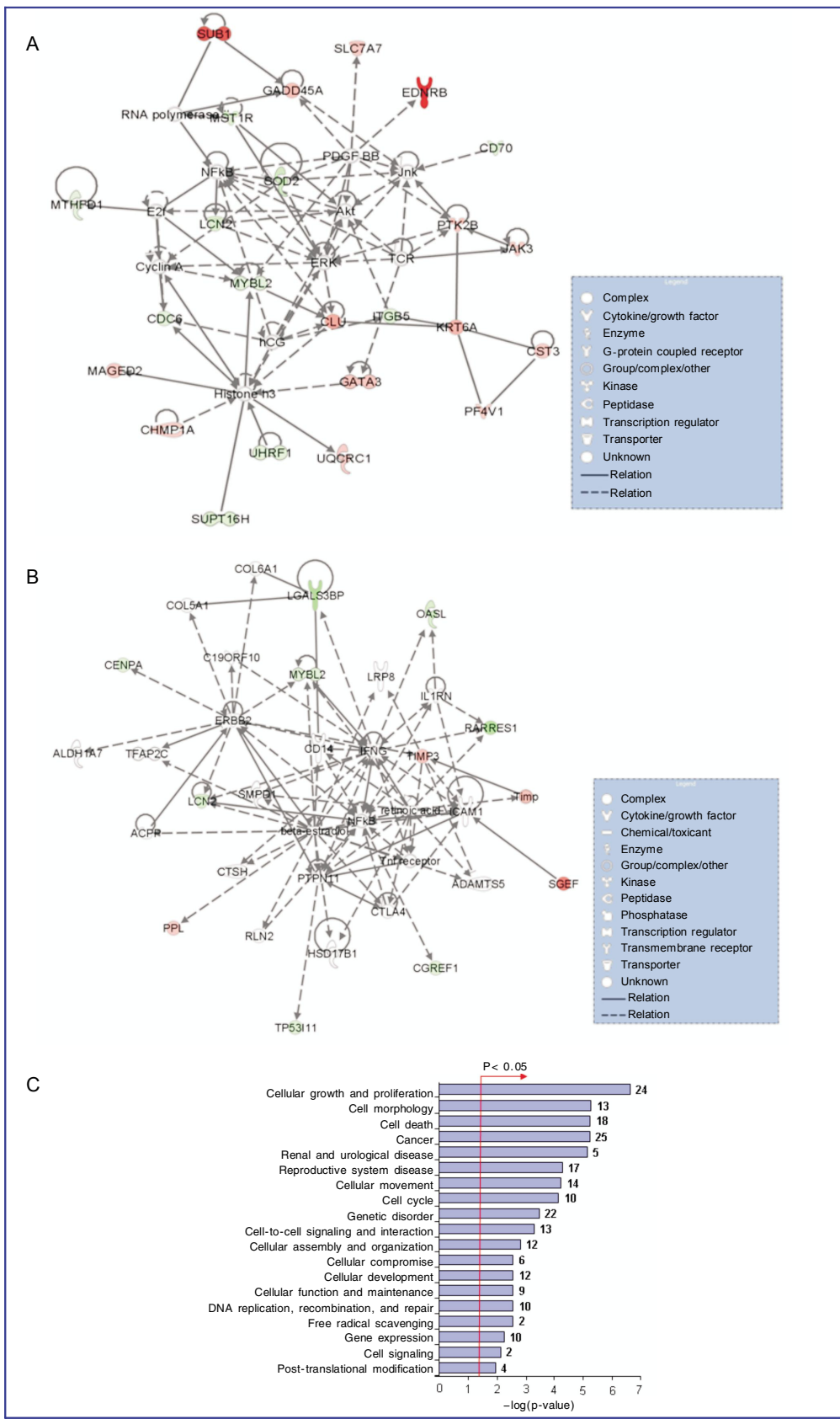
The multifunctional human transcriptional co-activator

SUB1 is a highly abundant nuclear protein that plays a key role in various cellular processes such as transcription, replication, chromatin organization, cellular transformation, and DNA damage repair^[10-13]. Previously, studies showed that *SUB1* was involved in p53-dependent transcriptional regulation to repair DNA damage. Recently, *SUB1* was found to play a direct role in the DNA double-stranded break (DSB) repair pathway through stimulation of DSB rejoining *in vivo*^[14,15]. High intensity ionizing radiation during spaceflight can damage DNA by directly interacting with DNA strands or indirectly promoting oxidative metabolism. Our study showed that *SUB1* was highly expressed in 48A9 cells after spaceflight. Together, these findings suggest that *SUB1* may play an important role in maintaining cellular homeostasis in spaceflight.

SUB1 maps to chromosome 5p13.3, a region frequently affected by loss of heterozygosity in bladder and lung tumors^[16,17]. *SUB1* can inhibit AP2 (activator protein 2) self-repression in a Ras-transformed cell line and act as a putative tumor suppressor^[18]. Ras oncogene-transformed cell lines that stably expressed *SUB1* cDNA had a diminished growth rate and a loss of anchorage-independent growth ability, and they were also unable to induce tumor formation in nude mice. In addition, *SUB1* acts as a unique activator of p53 by directly interacting with p53, activating p53-mediated DNA binding, and inducing p53-responsive gene expression^[19-21]. Thereby, *SUB1* plays an important role in the inhibition of tumorigenesis through interaction with p53. In our present study, *SUB1* was highly expressed in 48A9 cells compared with ground control cells, and thus, *SUB1* may be an important molecule in the change of biological function of 48A9 cells.

SGEF and its potential functions in 48A9 cells exposed to spaceflight

SGEF is a Rho GEF with unclear function. It was



initially discovered in a screening for androgen-responsive genes in human prostate, and two alternatively transcribed forms of *SGEF* gene were isolated. One encodes the full-length molecule of 871 amino acids, and the other encodes a splice-variant of 139 amino acids that contains only a small part of the pleckstrin homology (PH) domain and the entire SH3 domain^[22]. In addition, using an affinity-purified antibody of *SGEF*, a research group recently observed a variable presence of smaller immunoreactive proteins (90, 80, and 75 kDa) in a number of cell lines^[23]. These smaller proteins probably reflect that *SGEF* RNA is alternatively spliced to produce protein isoforms of varying functionality as described for the closely related exchange factor Rho guanine nucleotide exchange factor 5 (ARHGEF5)^[24].

The Rho GEFs activate Rho GTPases by displacing GDP from GDP-bound Rho GTPases and allowing GTP binding. Then, the activated Rho GTPases interact with downstream molecules to play an important role in the regulation of several aspects of cellular function, including cytoskeletal organization, apoptosis, gene expression, cell cycle progression, and membrane trafficking^[25-28]. RhoG, a Rho GTPase, has been reported to play a key role in controlling cell survival and apoptosis by activating the Akt pathway and JNK pathway, respectively^[29], in addition to its common roles as a Rho GTPase. In a recent study, *SGEF* was found to activate RhoG *in vitro* and *in vivo*^[22]. As a putative Rho GEF, we predict that *SGEF* influences cell morphology, cell apoptosis, and cell cycle through the regulation of RhoG.

Interestingly, a group recently identified a pathway downstream from ICAM1 involving RhoG and its exchange factor *SGEF* that led to endothelial apical cup formation and promoted leukocyte trans-endothelial migration (TEM)^[30]. In that study, ICAM1 bound to the SH3 domain of *SGEF* through the proline-rich region inside the cell. This interaction was independent of *SGEF* activation because catalytically inactive mutants of *SGEF* that expressed the SH3 domain still bound ICAM1. However, engagement of ICAM1 increased the activation of *SGEF*, as judged by increased binding of *SGEF* to nucleotide-free RhoG. In addition, previous studies have identified that spaceflight influenced the expression and spacial structure of ICAM1^[31-33]. Together, all these findings suggest that the pathway of ICAM1, *SGEF*, and RhoG possibly plays a key role in controlling cell morphology, cell survival, cell cycle, and gene expression during spaceflight.

SGEF mRNA was expressed at low levels in some breast and prostate cancer cell lines detected by Northern blot analysis^[21]. In our study, *SGEF* mRNA expression was not detected in normal Caski cancer cells but was highly expressed in 48A9 subclonal Caski cells. Combined with the findings from our previous

study^[6], this discovery may suggest that *SGEF* plays an important role in inhibiting oncogenesis.

***MALAT-1* and its potential functions in 48A9 cells exposed to spaceflight**

MALAT-1, a long non-coding RNA, is encoded by a gene locus located on human chromosome 11q13, where chromosomal aberrations associated with tumorigenesis and metastasis have long been observed. Moreover, some studies recently indicated that expression of the *MALAT-1* gene was increased in many human carcinomas and suggested a significant role for *MALAT-1* in the molecular events of oncogenesis^[34-36]. We found the expression level of *MALAT-1* was higher in 48A9 cells than in ground control cells. Therefore, further study should be undertaken to investigate whether *MALAT-1* acts as a tumor activator or tumor suppressor.

Among three new cDNAs or ESTs of unknown function, *B4* and *B5* were located on chromosome 3 and *C4* was located on chromosome 2. All three were highly expressed in 48A9 cells but not in ground control cells. Previous studies have indicated that the deletion of chromosome 3p is a common event in many cancers, including lung cancer, nasopharyngeal carcinoma, bladder cancer, and esophageal squamous cell carcinoma, suggesting that multiple tumor suppressor genes are present on chromosome 3p^[37-40]. To date, many candidate tumor suppressor genes at 3p have been reported, including Von Hippel-Lindau 3 (*VHL3*) at 3p25, retinoic acid receptor-beta (*RAR-β*) at 3p24, fragile histidine triad (*FHIT*) at 3p14.2, and Ras association (RalGDS/AF-6) domain family member 1 (*RASSF1A*), calcium channel, voltage-dependent, alpha 2/delta subunit 2 (*CACNA2D2*), and deleted in liver cancer 1 (*DLC1*) at 3p21.3^[41-46]. These findings suggest that our new clone *B5* on 3p23 may be a novel tumor suppressor gene.

Conclusions

The work described in the present study aimed to identify the causes of biological changes after spaceflight in cancer cells, expecting to find some new tumor suppressors. Though we have found genes and potential pathways impacted by spaceflight, there is a future challenge to establish their contributions to the associated biological changes. To our knowledge, our experiments are the first to show that spaceflight can reduce the growth of tumor cells and to provide a new model to study oncogenesis using a space environment.

Competing Interests

The authors of this study have no conflict of

interest or any financial disclosures to make.

Acknowledgments

This project has been supported in part by grants

from the National Nature Science Foundation of China (No. 30672352) and the 973 pre-major national basic research projects in China (No. CA04200).

Received: 2011-04-25; revised: 2011-08-01;
accepted: 2011-10-31.

References

- [1] Allen DL, Bandstra ER, Harrison BC, et al. Effects of spaceflight on murine skeletal muscle gene expression [J]. *J Appl Physiol*, 2009,106(2):582–895.
- [2] Bascope M, Huin-Schohn C, Guéguinou N, et al. Spaceflight-associated changes in immunoglobulin VH gene expression in the amphibian *Pleurodeles waltl* [J]. *FASEB J*, 2009,23(5):1607–1615.
- [3] Gridley DS, Slater JM, Luo-Owen X, et al. Spaceflight effects on T lymphocyte distribution, function and gene expression [J]. *J Appl Physiol*, 2009,106(1):194–202.
- [4] Ou X, Long L, Zhang Y, et al. Spaceflight induces both transient and heritable alterations in DNA methylation and gene expression in rice (*Oryza sativa* L.) [J]. *Mutat Res*, 2009,662(1–2):44–53.
- [5] Salmi ML, Roux SJ. Gene expression changes induced by space flight in single-cells of the fern *Ceratopteris richardii* [J]. *Planta*, 2008,229(1):151–159.
- [6] Yang C, Li YH, Zhang ZJ, et al. Effects of space flight exposure on cell growth, tumorigenicity and gene expression in cancer cells [J]. *Adv Space Res*, 2008,42(12):1898–1905.
- [7] Hillmann A, Dunne E, Kenny D. cDNA amplification by SMART-PCR and suppression subtractive hybridization (SSH)-PCR [J]. *Methods Mol Biol*, 2009,496:223–243.
- [8] Cao W, Epstein C, Liu H, et al. Comparing gene discovery from Affymetrix GeneChip microarrays and Clontech PCR-select cDNA subtraction: a case study [J]. *BMC Genomics*, 2004,5(1):26.
- [9] Diatchenko L, Lukyanov S, Lau YF, et al. Suppression subtractive hybridization: a versatile method for identifying differentially expressed genes [J]. *Methods Enzymol*, 1999,303:349–380.
- [10] Das C, Hizume K, Batta K, Kumar BR, et al. Transcriptional coactivator PC4, a chromatin-associated protein, induces chromatin condensation [J]. *Mol Cell Biol*, 2006,26(22):8303–8315.
- [11] Wang JY, Sarker AH, Cooper PK, et al. The single-strand DNA binding activity of human PC4 prevents mutagenesis and killing by oxidative DNA damage [J]. *Mol Cell Biol*, 2004,24(13):6084–6093.
- [12] Pan ZQ, Ge H, Amin AA, et al. Transcription-positive cofactor 4 forms complexes with HSSB (RPA) on single-stranded DNA and influences HSSB-dependent enzymatic synthesis of simian virus 40 DNA [J]. *J Biol Chem*, 1996,271(36):22111–22116.
- [13] Ge H, Roeder RG. Purification, cloning, and characterization of a human coactivator, PC4, that mediates transcriptional activation of class II genes [J]. *Cell*, 1994,78(3):513–523.
- [14] Batta K, Yokokawa M, Takeyasu K, et al. Human transcriptional coactivator PC4 stimulates DNA end joining and activates DSB repair activity [J]. *J Mol Biol*, 2009,385(3):788–799.
- [15] Mortusewicz O, Roth W, Li N, Cardoso MC, et al. Recruitment of RNA polymerase II cofactor PC4 to DNA damage sites [J]. *J Cell Biol*, 2008,183(5):769–776.
- [16] Bohm M, Kirch H, Otto T, et al. Deletion analysis at the DEL-27, APC and MTS1 loci in bladder cancer: LOH at the DEL-27 locus on 5p13-12 is a prognostic marker of tumor progression [J]. *Int J Cancer*, 1997,74(3):291–295.
- [17] Wieland I, Bohm M, Arden KC, et al. Allelic deletion mapping on chromosome 5 in human carcinomas [J]. *Oncogen*, 1996,12(1):97–102.
- [18] Kannan P, Tainsky MA. Coactivator PC4 mediates AP-2 transcriptional activity and suppresses ras-induced transformation dependent on AP-2 transcriptional interference [J]. *Mol Cell Biol*, 1999,19(1):899–908.
- [19] Kishore AH, Batta K, Das C, et al. p53 regulates its own activator: transcriptional co-activator PC4, a new p53-responsive gene [J]. *Biochem J*, 2007,406(3):437–444.
- [20] Batta K, Kundu TK. Activation of p53 function by human transcriptional coactivator PC4: role of protein-protein interaction, DNA bending, and posttranslational modifications [J]. *Mol Cell Biol*, 2007,27(21):7603–7614.
- [21] Banerjee S, Kumar BR, Kundu TK. General transcriptional coactivator PC4 activates p53 function [J]. *Mol Cell Biol*, 2004,24(5):2052–2062.
- [22] Qi H, Fournier A, Grenier J, et al. Isolation of the novel human guanine nucleotide exchange factor Src homology 3 domain-containing guanine nucleotide exchange factor (SGEF) and of C-terminal SGEF, an N-terminally truncated form of SGEF, the expression of which is regulated by androgen in prostate cancer cells [J]. *Endocrinology*, 2003,144(5):1742–1752.
- [23] Ellerbroek SM, Wennerberg K, Arthur WT, et al. SGEF, a RhoG guanine nucleotide exchange factor that stimulates macropinocytosis [J]. *Mol Biol Cell*, 2004,15(7):3309–3319.
- [24] Debily MA, Camarca A, Ciullo M, et al. Expression and molecular characterization of alternative transcripts of the ARHGEF5/TIM oncogene specific for human breast cancer [J]. *Hum Mol Genet*, 2004,13(3):323–334.
- [25] Sahai E, Marshall CJ. RHO-GTPases and cancer [J]. *Nat Rev Cancer*, 2002,2(2):133–142.
- [26] Etienne-Manneville S, Hall A. Rho GTPases in cell biology [J]. *Nature*, 2002,420(6916):629–635.
- [27] Hall A. Rho GTPases and the actin cytoskeleton [J]. *Science*, 1998,279(5350):509–514.
- [28] Van Aelst L, D'Souza-Schorey C. Rho GTPases and signaling networks [J]. *Genes Dev*, 1997,11(18):2295–2322.
- [29] Murga C, Zohar M, Teramoto H, et al. Rac1 and RhoG promote cell survival by the activation of PI3K and Akt, independently of their ability to stimulate JNK and NF-kappaB [J]. *Oncogene*, 2002,21(2):207–216.
- [30] van Buul JD, Allingha MJ, Samson T, et al. RhoG regulates endothelial apical cup assembly downstream from ICAM1 engagement and is involved in leukocyte trans-endothelial migration [J]. *J Cell Biol*, 2007,178(7):1279–1293.
- [31] Buravkova L, Romanov Y, Rykova M, et al. Cell-to-cell interactions in changed gravity: ground-based and flight experiments [J]. *Acta Astronaut*, 2005,57(2–8):67–74.
- [32] Jung CK, Chung S, Lee YY, et al. Monocyte adhesion to endothelial cells increases with hind-limb unloading in rats [J]. *Aviat Space Environ Med*, 2005,76(8):720–725.

- [33] Mills PJ, Perez CJ, Adler KA, et al. The effects of spaceflight on adrenergic receptors and agonists and cell adhesion molecule expression [J]. *J Neuroimmunol*, 2002,132(1-2):173-179.
- [34] Lin R, Maeda S, Liu C, et al. A large noncoding RNA is a marker for murine hepatocellular carcinomas and a spectrum of human carcinomas [J]. *Oncogene*, 2007,26 (6):851-858.
- [35] Ji P, Diederichs S, Wang W, et al. MALAT-1, a novel noncoding RNA, and thymosin beta4 predict metastasis and survival in early-stage non-small cell lung cancer [J]. *Oncogene*, 2003,22(39):8031-8041.
- [36] Yamada K, Kano J, Tsunoda H, et al. Phenotypic characterization of endometrial stromal sarcoma of the uterus [J]. *Cancer Sci*, 2006,97(2):106-112.
- [37] Fang Y, Guan X, Guo Y, et al. Analysis of genetic alterations in primary nasopharyngeal carcinoma by comparative genomic hybridization [J]. *Genes Chromosomes Cancer*, 2001,30 (3): 254-260.
- [38] Hurst CD, Fiegler H, Carr P, et al. High-resolution analysis of genomic copy number alterations in bladder cancer by microarray-based comparative genomic hybridization [J]. *Oncogene*, 2004,23(12):2250-2263.
- [39] Qin YR, Fu L, Sham PC, et al. Single-nucleotide polymorphism-mass array reveals commonly deleted regions at 3p22 and 3p14.2 associate with poor clinical outcome in esophageal squamous cell carcinoma [J]. *Int J Cancer*, 2008,123(4):826-830.
- [40] Tai AL, Yan WS, Fang Y, et al. Recurrent chromosomal imbalances in nonsmall cell lung carcinoma: the association between 1q amplification and tumor recurrence [J]. *Cancer*, 2004,100(9):1918-1927.
- [41] Daigo Y, Nishiwaki T, Kawasoe T, et al. Molecular cloning of a candidate tumor suppressor gene, DLC1, from chromosome 3p21.3 [J]. *Cancer Res*, 1999,59(8):1966-1972.
- [42] Dammann R, Li C, Yoon JH, et al. Epigenetic inactivation of a RAS association domain family protein from the lung tumour suppressor locus 3p21.3 [J]. *Nat Genet*, 2000,25(3):315-319.
- [43] de The H, Vivanco-Ruiz MM, Tiollais P, et al. Identification of a retinoic acid responsive element in the retinoic acid receptor beta gene [J]. *Nature*, 1990,343(6254):177-180.
- [44] Ji L, Nishizaki M, Gao B, et al. Expression of several genes in the human chromosome 3p21.3 homozygous deletion region by an adenovirus vector results in tumor suppressor activities in vitro and in vivo [J]. *Cancer Res*, 2002,62(9):2715-2720.
- [45] Latif F, Tory K, Gnarr J, et al. Identification of the von Hippel-Lindau disease tumor suppressor gene [J]. *Science*, 1993,260 (5112):1317-1320.
- [46] Ohta M, Inoue H, Cotticelli MG, et al. The FHIT gene, spanning the chromosome 3p14.2 fragile site and renal carcinoma-associated t(3;8) breakpoint, is abnormal in digestive tract cancers [J]. *Cell*, 1996,84(4):587-597.